Absorption of Self-Propelled Particles into Dense Porous Medium

Supplementary Information

Bing-shuang Qian,[a] Wen-de Tian,[a] and Kang Chen*[ab]

[a]Center for Soft Condensed Matter Physics & Interdisciplinary Research, School of Physical Science and Technology, Soochow University, Suzhou 215006, China

[b]School of Physics and Information Engineering, Shanxi Normal University, Linfen 041004, China

*Corresponding authors: kangchen@suda.edu.cn (K.C.)

Dynamics of a single Self-Propelled Particle (SPP) in the periodic square obstacle array

Here we explore the motion of a single SPP in an infinite dense medium mimicked by periodic square obstacle array.[1,2] All interactions, units and equation of motions are set the same as in the main text. The lattice constant $a = 1.9\sigma$, hence a barrier of $E_b \sim 5.29 k_B T$ blocks the motion of the SPP passing through the middle between two adjacent obstacles as shown in Fig. 2(a).
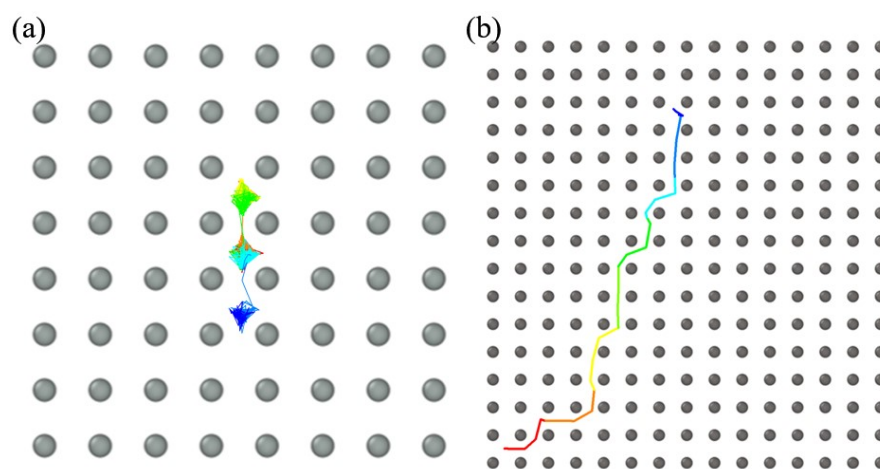

Fig. S1 Typical single-particle trajectory. (a) $F_a = 5$ and $D_r = 0.001$; (b) $F_a = 30$ and $D_r = 0.001$. The color represents the time sequence of the trajectory (starting from blue).

1. Barrier-hopping dynamics vs. smooth crossing

Propelling force could enhance the transport of SPPs in the dense obstacle array as manifested in Fig. 1. When the propelling strength is not large enough, e.g. $F_a = 5$, thermal activation is still needed for the SPP to overcome the barrier. Correspondingly, the SPP is temporarily

localized or caged by surrounding obstacles and escapes by barrier-hopping process (Fig. S1(a)). In contrast, smooth motion is recovered when the propelling strength is very large, e.g. $F_a = 30$ (Fig. S1(b)).
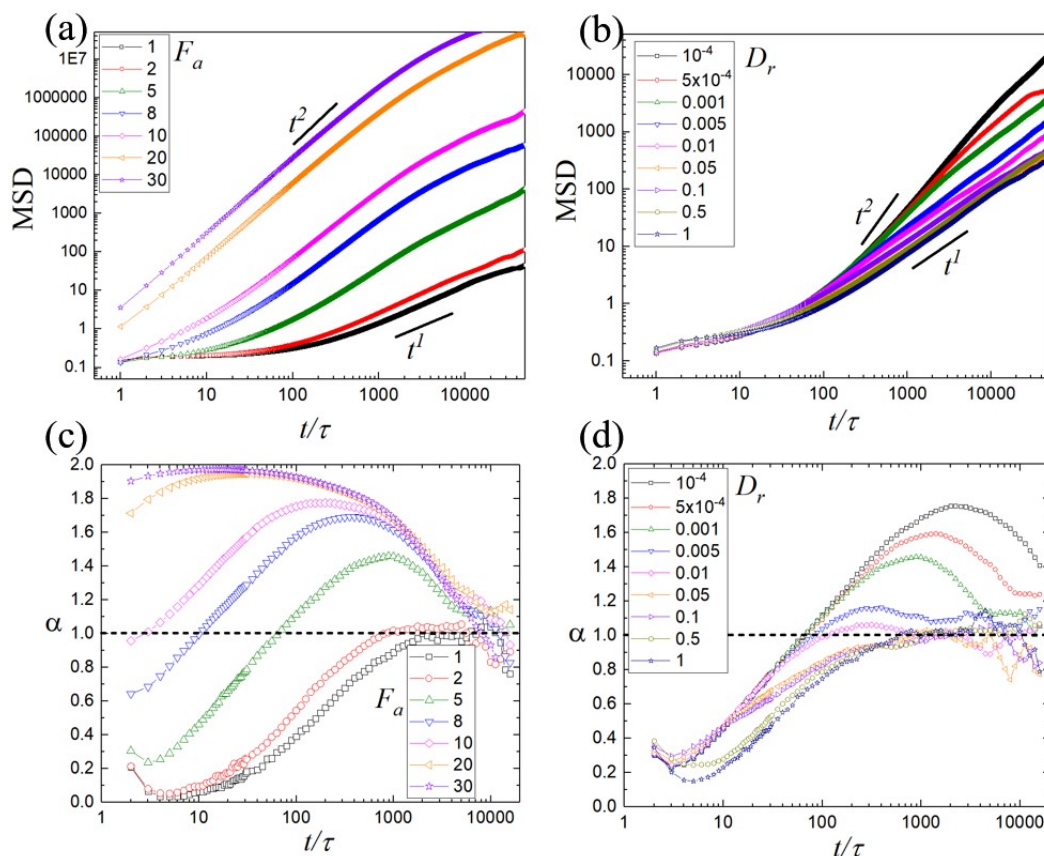

Fig. S2 Mean squared displacement (MSD) of a single SPP in the obstacle array for (a) varied F_a and $D_r = 0.001$; (b) varied D_r and $F_a = 5$. The corresponding time-dependent exponent is shown in (c) and (d).

2. Mean Squared Displacement (MSD)

F_a and D_r are two key parameters characterizing the active motion of a SPP in free space. Here, we calculate the MSD of a single SPP moving in the obstacle array under various F_a's (Fig. S2(a)) and D_r's (Fig. S2(b)). For $F_a \leq 10$ in Fig. S2(a), the early part of the MSD increases slowly with time, reflecting the caging dynamics. Then the MSD curves upwardly and the exponent α ($MSD \sim t^\alpha$) increases (Fig. S2(c)), corresponding to the process of the SPP escaping the cage. At low propelling strength, e.g. $F_a = 1$ and 2, α reaches the maximum ~1,

i.e. the dynamics changes directly from caging at early time to normal diffusion at late time. In contrast, an intermediate super-diffusive region (i.e. $\alpha > 1$) appears, bridging the early caging regime and the late normal diffusive regime, when the propelling strength is moderate ($5 \leq F_a \leq 10$ in Fig. S2(a) and (c)). For very strong propulsion, e.g. $F_a = 20$ and 30, the MSD starts with the super-diffusive dynamics with α approaching 2 without the caging regime in the beginning. Correspondingly, the transport behavior of the SPP becomes smooth (Fig. S1(b)). At long time $t \gg 1/D_r$ (i.e. $t \gg 1000\tau$), all MSD curves recover the normal diffusion behavior $\alpha \sim 1$.

Similar caging regime and the following super-diffusive and/or normal diffusive regimes are observed for the MSD curves under different D_r's (Fig. S2(b) and (d)). The super-diffusive regime disappears at large D_r (e.g. $D_r \geq 0.05$), presumably because the time scale of localization becomes exceeding the time scale for the transition to the normal diffusion.
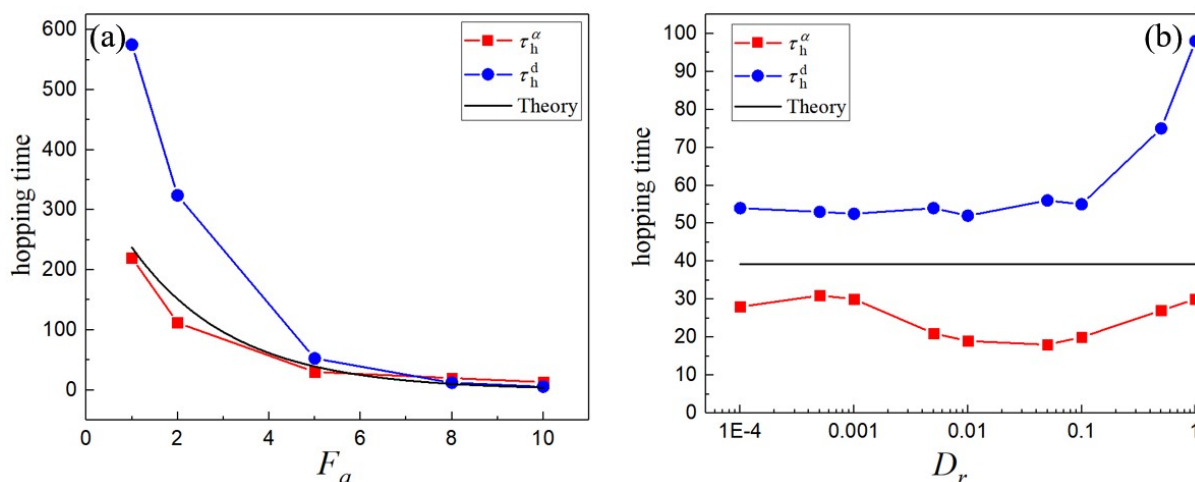

Fig. S3 Hopping time as a function of (a) F_a ($D_r = 0.001$) and (b) D_r ($F_a = 5$).

3. Characteristic time scales

In the above, we see the transitions from caging dynamics to super-diffusion and/or to normal diffusion of the MSD of a single SPP in the obstacle array. These transitions depend on the time scales. In free space, the MSD of an overdamped single SPP shows a transition from super-diffusion ($\alpha = 2$) at early time to normal diffusion ($\alpha = 1$) at late time. The characteristic

time scale for this transition is the persistence time of propulsion $1/D_r$. In the dense obstacle array (and $F_a \leq 10$ in our model), a hopping time (or caging time) τ_h characterizes the time scale for the SPP to escape a local cage. If $1/D_r \gg \tau_h$, the MSD curve changes firstly from caging dynamics to super-diffusion around τ_h and then to normal diffusion around $1/D_r$. On the contrary, the intermediate super-diffusive regime disappears when τ_h approaches or even exceeds $1/D_r$.

We adopt two ways to quantify the hopping time τ_h. In one way, we calculate the second derivative of the log-log MSD curve around the transition from caging dynamics to super- or normal diffusion. We denote the time when the second derivative reaches maximum as the hopping time τ_h^α. Alternatively, we choose the time when the MSD reaches the square of half lattice constant, $a^2/4$, as the hopping time τ_h^d. The results are shown in Fig. S3. The theoretical hopping time based on the Eyring's model, $\tau e^{(E_b - F_a L_b)/k_B T}$ with $L_b = 0.45\sigma$ is also shown for comparison. The three hopping times agree well with each other when the persistence time $1/D_r > 10$ and the propelling strength is moderate, e.g. $5 \leq F_a \leq 10$.

Table S1 Effective temperatures and corresponding hopping times for varied F_a ($D_r = 0.001$).

F_a	1	2	5	8	10	20	30
T_v/T	1	1	1.005	1.01	1.035	1.735	3.355
τ_h/τ	372	372	362	351	305	30	6
T_U/T	0.27	0.29	0.45	0.74	0.98	2.1	2.5
τ_h/τ	3×10^9	7×10^8	5×10^5	2981	420	17	11
T_{free}/T	1.005	1.02	1.125	1.32	1.5	3	5.5
τ_h/τ	362	332	193	88.7	51.8	7.2	2.93

Table S2 Effective temperatures and corresponding hopping times for varied D_r ($F_a = 5$).

D_r	10^{-4}	0.0005	0.001	0.005	0.01	0.05	0.1	0.5	1
T_v/T	1	1	1.005	1.005	1.005	1.005	1.005	1.025	1.035
τ_h/τ	372	372	362	362	362	362	362	322	304
T_U/T	0.453	0.453	0.453	0.453	0.452	0.446	0.442	0.412	0.387
τ_h/τ	5×10^5	5×10^5	5×10^5	5×10^5	5×10^5	6×10^5	7×10^5	2×10^6	4×10^6
T_{free}/T	1.125	1.125	1.125	1.125	1.125	1.124	1.124	1.119	1.114
τ_h/τ	193	193	193	193	193	193	193	198	204

4. Effective temperatures

Researchers favor using the concept of effective temperature to map the nonquilibrium active system to a thermal passive one. For example, effective temperatures based on average potential energy and average kinetic energy are defined to formulate the mean escape time of an active particle in a harmonic trap.[3] Motivated by the reference paper,[3] we calculate statistically, under various conditions, the effective temperatures based on the particle's average kinetic energy (T_v) and average potential energy (T_U) in the obstacle array. And, for comparison, we also present the effective temperature of the same SPP in free space (T_{free}), based on its average kinetic energy. For the Langevin equation with mass term, we have, for a free SPP, $v_{free}^2 = v_a^2/(1 + \tau_m D_r) + 2k_B T/m$, with $v_a = F_a/\zeta$ the propulsion speed and $\tau_m = m/\zeta$ the momentum relaxation time. We then obtain the mean hopping times by replacing the thermal temperature in the Kramers' expression by the effective temperatures, i.e. $\tau_h = \tau e^{E_b/k_B T_{eff}}$. The results are summarized in Table S1 and S2. We see that the impact of propulsion on T_v is negligible when $F_a \leq 10$, and T_U is even lower than the thermal temperature. Correspondingly, we get unreasonably large hopping times. This suggests that the effective-temperature description of a SPP transporting in the complex potential landscape of a two-dimensional array does not work. More importantly, in the situation of many particles and finite obstacle array, the aggregation of SPPs is a purely nonequilibrium dynamic phenomenon. We won't have tight aggregation of particles in the obstacle array in the passive

thermal picture even if the effective temperature is high and the barrier-hopping dynamics is strongly accelerated.

5. Effective propulsion speed

In free space, the (two-dimensional) MSD of an overdamped single SPP follows[4]

$$MSD = 2Dt + \frac{2v_a^2}{D_r}\left[t + \frac{1}{D_r}\left(e^{-D_r t} - 1\right)\right],$$

(S1)

where $D = k_B T/\zeta$ is the thermal diffusion constant. We can use this formula to fit the MSD of a single SPP in the obstacle array at long time limit by replacing v_a by effective propulsion speed v_a^{eff}.[5] Figure S4 shows the scaled v_a^{eff}/v_a as a function of F_a and D_r. Apparently, v_a^{eff} is lower than v_a, which becomes more prominent at smaller F_a and D_r. Therefore, for many SPPs in the obstacle array, the slowing down of motion arises not only by particle collisions but also enhanced by potential barriers. Such slowing down of motion brings about the aggregation or clustering of SPPs around the obstacle array analogous to the phenomenon of motility-induced phase separation but happening at lower concentration threshold.
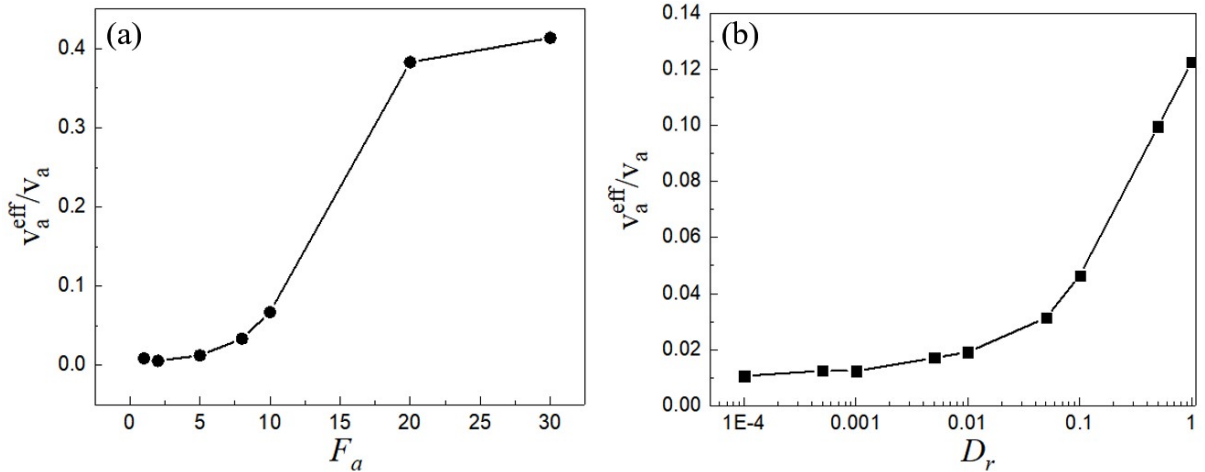

Fig. S4 Scaled effective propulsion speed as a function of (a) F_a ($D_r = 0.001$) and (b) D_r ($F_a = 5$).

References

1 M. Zeitz, K. Wolff and H. Stark, *Eur. Phys. J. E*, 2017, **40**, 23.
2 S. Pattanayak, R. Das, M. Kumar and S. Mishra, *Eur. Phys. J. E*, 2019, **42**, 62.

3 D. Wexler, N. Gov, K. Ø. Rasmussen and G. Bel, *Phys. Rev. Res.*, 2020, **2**, 013003.

4 C. Bechinger, R. Di Leonardo, H. Löwen, C. Reichhardt, G. Volpe and G. Volpe, *Rev. Mod. Phys.*, 2016, **88**, 045006.

5 M. E. Cates and J. Tailleur, *Annu. Rev. Condens. Matter Phys.*, 2015, **6**, 219–244.